Geodesy and Geodynamics 2013,4(4):33-40

http://www.jgg09.com
Doi:10.3724/SP.J.1246.2013.04040

Temporal distribution characteristics of GNSS ionospheric occultation data and its effects in earthquake-ionosphere anomaly detection

Zhao Ying[1] and An Jiachun[2]

[1] *Key Laboratory of Earthquake Geodesy, Institute of Seismology, China Earthquake Administration, Wuhan* 430071, *China*

[2] *Chinese Antarctic Center of Surveying and Mapping, Wuhan University, Wuhan* 430079, *China*

Abstract: The temporal distribution characteristics of COSMIC occultation data are analyzed in detail, and the limitations in earthquake-ionosphere anomaly detection caused by the temporal distribution characteristics of COSMIC occultation data are discussed using the example of the Wenchuan earthquake. The results demonstrate that there is no fixed temporal resolution for COSMIC occultation data when compared with other ionospheric observation techniques. Therefore, occultation data cannot currently be independently utilized in research studies but can only be used as a complement to other ionospheric observation techniques for applications with high temporal resolution demands, such as earthquake-ionosphere anomaly detection.

Key words: GNSS; radio occultation; ionosphere; temporal distribution characteristics; earthquake

1 Introduction

One of the methods used to predict earthquakes is to obtain earthquake precursory information using the scientific method. It has been widely discussed in the literature that many electromagnetic phenomena may be linked to seismic activity[1-4], and existing research results demonstrate that the earthquake process can also be reflected in the electromagnetic fields in the ionosphere[5-7]. Scientists have found that some ionospheric anomalies, often referred to as earthquake-ionospheric effects, may occur a few days before large earthquakes in the F layer. Twenty magnitude 6.0 earthquakes in Taiwan that occurred between 1999 to 2002 have been analyzed by Liu[1]. The results indicate that there are obvious ionospheric anomalies 5 days before the earthquakes, especially in the 18:00-22:00 LT (local time) period. These ionospheric anomalies typically occur specifically 2-5 days before the earthquake and that anomalies are always negative with downward trending VTEC values[8].

Ionospheric sounding techniques include several traditional methods, such as ionosonde, GPS and incoherent scatter radar (ISR); however, these methods can only sample the ionospheric electron content or electron density over a localized station and are restricted by the geographical environment, especially in ocean, polar and other special areas. Therefore, a new ionospheric sounding technology, radio occultation detection, came into being. This technique originated in the mid-1960s and was first used to study the atmosphere and ionosphere of the planets in our solar system by JPL(Jet Propulsion Laboratory) and Stanford University. With the success of the GPS/MET occultation exploration program in 1995, this technology became widely used in the detection of Earth's neutral atmosphere and ionosphere[9]. GNSS ionospheric occultation inversion has many advantages, such as all-weather global coverage, high vertical resolution, near real-

Received:2013-03-11; Accepted:2013-06-28

Corresponding author: An Jiachun, E-mail: jcan@whu.edu.cn

This study is supported by the National Science Foundation of China (41174029, 41204028), Chinese Arctic and Antarctic Administration (20110205), and the Fundamental Research Funds for the Central Universities (121001).

time and self-calibration, which other ionospheric sounding methods lack. In particular, this technology can also make up for the lack of ionospheric observational data for special areas, such as ocean and polar areas, and provide more information and more choices for ionospheric research[10].

To detect earthquake-ionospheric effects, the ionosphere data for several continuous days at a fixed location must be compared. In terms of the currently available ionospheric sounding methods, the sampling rate of the ionosonde is 15 minutes, and the IONEX provided by IGS has a data sampling period of 2 hours. All these data can be used to make an analysis of the continuous changes in the ionosphere over the observation site. GNSS ionospheric occultation inversion can achieve a global distribution with a higher vertical resolution; however, its horizontal and temporal resolutions are very low, which bring a certain limitation to its application.

The temporal distribution characteristics of the COSMIC occultation data are analyzed in detail, and the limitations of earthquake-ionosphere anomaly detection, which are caused by the temporal distribution characteristics of the COSMIC occultation data, are discussed using the example of the Wenchuan earthquake.

2 COSMIC occultation observations and temporal distribution characteristics

Any two occultation events whose latitude and longitude differ by less than 2° and that occur in one day are defined as a repeat occultation events at that location. The occultation data from day 244 to day 247 in 2009 are selected, and their occultation temporal distribution characteristics are analyzed with regard to two aspects: the number of occultation events on one day and the distribution of repeat occultation events with regards to the time interval.

2.1 The number of occultation events on one day

Figure 1 shows the distribution of occultation events from day 244 to day 247 in 2009 all over the world. Abundant occultation events occurred on one day, and these events achieved a global uniform distribution; however, this advantage no longer existed when the time interval was reduced to approximately 1 hour, as shown in figures 2 and 3.

Figure 2 shows the global distribution of occultation events (successfully inverted) that occurred at UT02:00, UT08:00, UT14:00 and UT20:00 from day 244 to day 247, respectively. Figure 3 provides the statistical average number of occultation events that occurred every hour in September 2009, where blue indicates the number of all occultation events and red indicates the occultation events that can be successfully inverted.

This figure shows that there are approximately 90 occultation events per hour in 1 day and that approximately 60 of these events can be successfully inverted. Whereas there is no rule for the location of the occultation

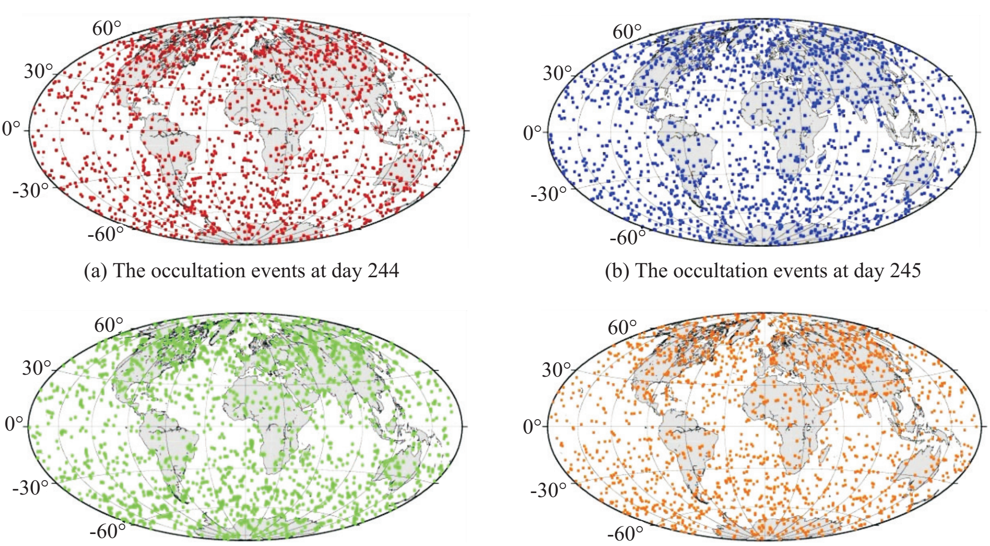

(a) The occultation events at day 244

(b) The occultation events at day 245

(c) The occultation events at day 246

(d) The occultation events at day 247

Figure 1 Distribution of occultation events from day 244 to day 247 in 2009 events, the number of matching occultation events occurring on 2 days or on several continuous days at the same time in a similar position is not significant.

2.2 Distribution of the number of repeat occultation events with time intervals

All of the occultation events that occurred from day 244 to day 247 are selected for analysis, and the distribution of the number of repeated occultation events with the time intervals is discussed. The number of repeated occultation events that occurred from day 244 to day 247 is shown in table 1, and the number of repeated occultation events that occurred at the same place is at a maximum of 5 times during these 4 days.

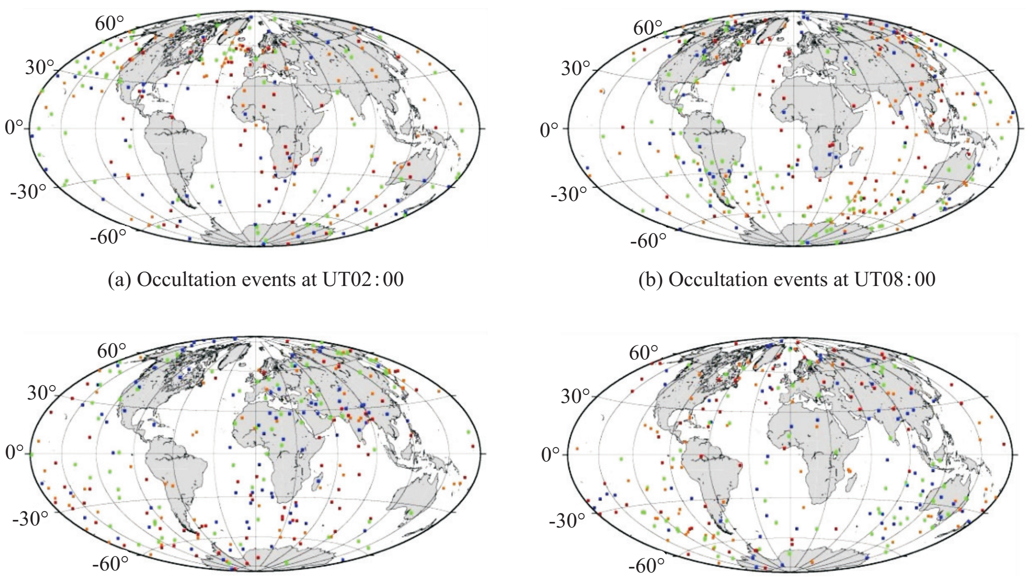

(a) Occultation events at UT02:00 (b) Occultation events at UT08:00 (c) Occultation events at UT14:00 (d) Occultation events at UT20:00

Figure 2 Distribution of occultation events at different times (red indicates day 244, blue indicates day 245, green indicates day 246, and orange indicates day 247)

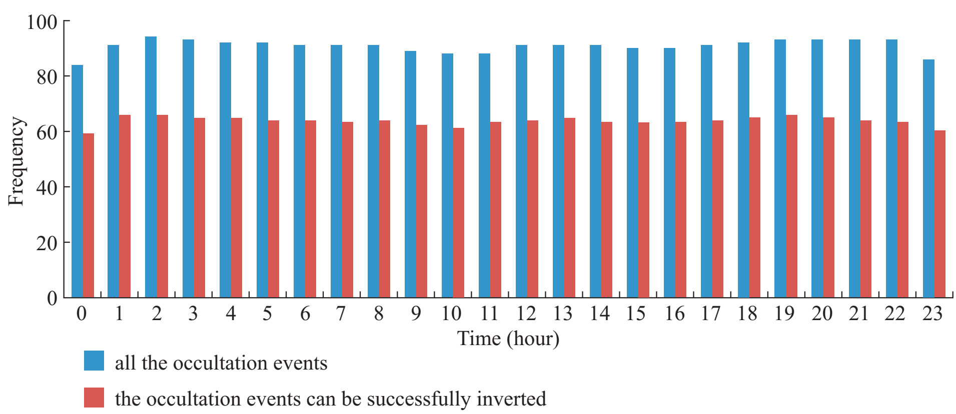

Figure 3 Statistics for the average number of occultation events that occurred every hour in September 2009

Table 1 The number of repeated occultation events that occurred from day 244 to day 247, 2009

	244	245	246	247
The number of repeated occultation events	324	298	373	362
The maximum number of repeated occultation events that occurred at the same place	5	3	4	3

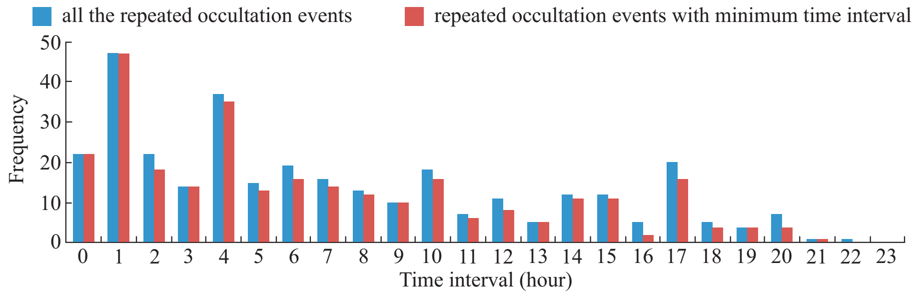

(a) The repeated occultation events at day 244 in 2009

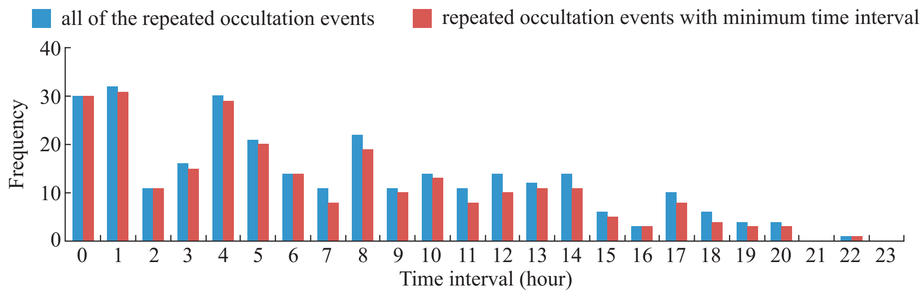

(b) The repeated occultation events at day 245 in 2009

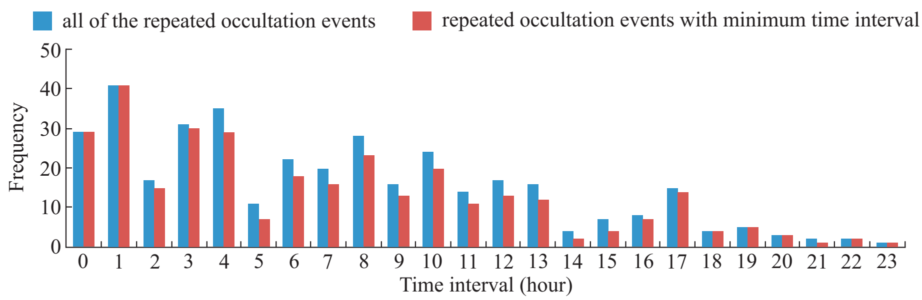

(c) The repeated occultation events at day 246 in 2009

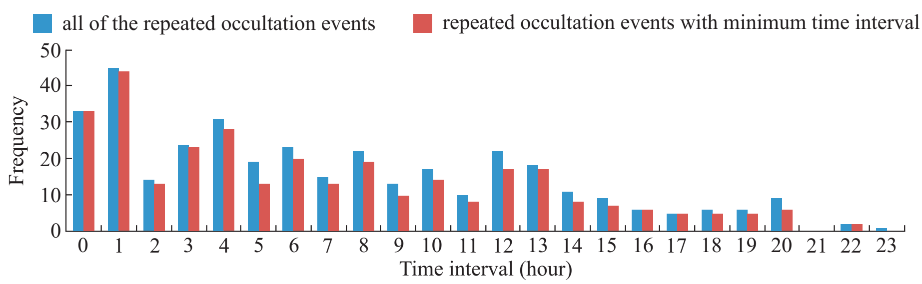

(d) The repeated occultation events at day 247 in 2009

Figure 4 The frequency of repeated occultation events that occurred at different time intervals from day 244 to day 247 in 2009

Figure 4 provides the frequency of the repeated occultation events that occurred at different time intervals from day 244 to day 247 in 2009 (the first repeated occultation event occurred in every location) during the different time intervals. Figure 5 shows the percentage of repeated occultation events with a minimum time interval during different time intervals from day 244 to day 247 in 2009. Figure 6 shows the global distribution of repeated occultation events for these 4 days.

As can be observed in these figures, there is no regularity for the number of repeated occultation events in the different time intervals. However, the statistical results of these 4 days indicate that the number of repeated occultation events is significantly more during the time interval 00:00–03:00, at an average of approximately 35%. The number of repeated occultation events is not in the minority when the time interval is longer than 15 hours. These data demonstrate that the time interval for the repeated occultation events is different in different locations on one day and that there is no rule for the location of the repeated occultation events. Therefore, there is no fixed temporal resolution for the

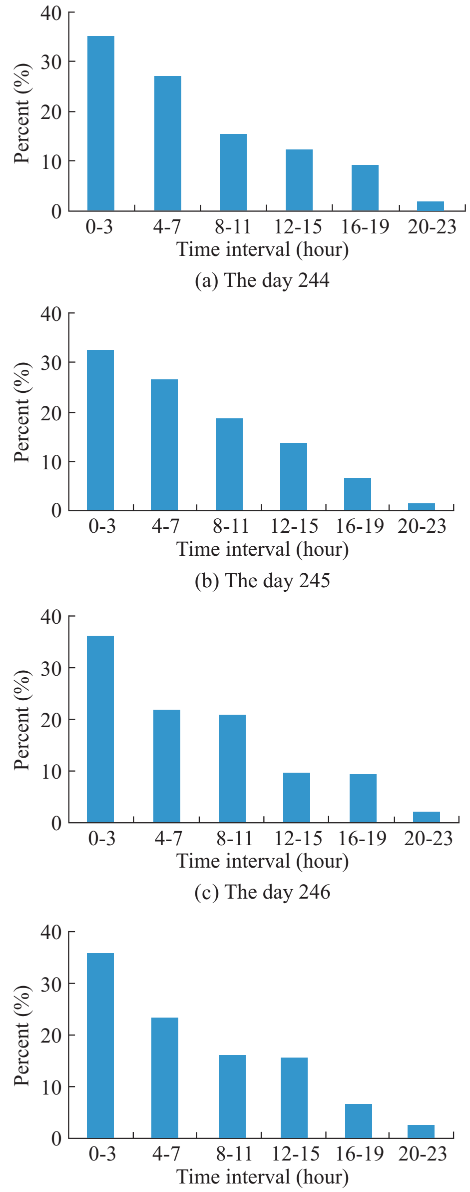

(a) The day 244
(b) The day 245
(c) The day 246
(d) The day 247

Figure 5 Percentage of repeated occultation events with a minimum time interval that occurred during different time intervals in 2009

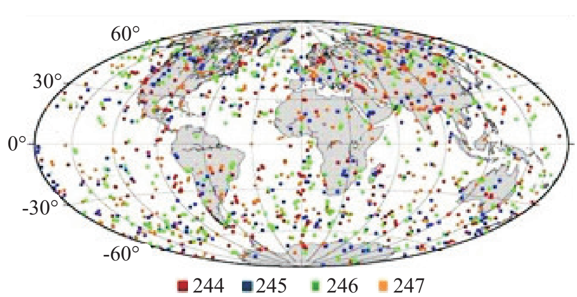

Figure 6 Distribution of repeated occultation events from day 244 to day 247 in 2009

COSMIC occultation data. Overall, compared to other traditional ionospheric techniques, the temporal resolution of ionospheric occultation inversion is very low.

3 The impact of the temporal distribution characteristics of the COSMIC occultation data on earthquake-ionosphere anomaly detection

A low temporal resolution is likely to influence the application of occultation data. Taking the Wenchuan earthquake (epicenter location: 30.986°N, 103.364°E) as an example, in this paper we discuss the impact of the temporal distribution characteristics of the COSMIC occultation data on earthquake−ionosphere anomaly detection, which is caused by the temporal distribution characteristics of COSMIC occultation data provided by UCAR.

For the COSMIC ionospheric occultation data, 8 days of data before the earthquake are selected with the longitude and latitude being ± 10° and ± 3°, respectively. There are a few occultation events in the defined area from May 4 to May 12, 2008, with most of them concentrated in LT00:00−05:00 and LT18:00−23:00 (Fig.7). The picture shows the distribution of occultation events near the epicenter from May 4 to May 12 LT00:00−05:00 and LT18:00−23:00. It can be observed that due to the low resolution, the number of occultation events during the two periods is not significant and that the time and location of the occultation events are different every day. Therefore, we cannot usually choose the statistical methods used for analyzing the IGS VTEC observations and can only compare a single occultation event at two different time regions in

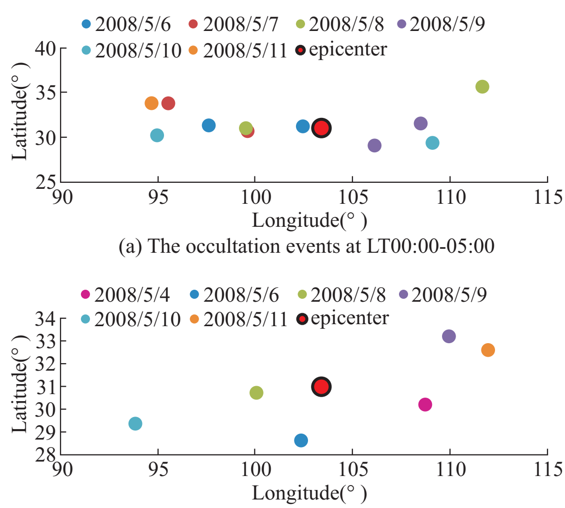

(a) The occultation events at LT00:00-05:00
(b) The occultation events at LT18:00-23:00

Figure 7 Distribution of occultation events near the epicenter the selected area from May 4 to May 12, 2011.

Figure 8 shows the corresponding electron density profiles and occultation tangential point loci of the occultation events near the epicenter from May 4 to May 12, 2008, LT18:00-23:00 (May 5, May 7 and May 12 had no occultation events in this region). Figure 8(a) are the results of the electron density profiles. There is a substantial decrease of the F2 layer peak density on May 6, 8 and 10 when compared with May 4. The maximum reduction is approximately 8×10^4 el/cm^3.

Figure 9 shows the corresponding electron density profiles and the occultation tangential point loci of the occultation events near the epicenter on May 4-12, LT00:00-05:00 (May 4 and May 11 had no occultation events in this region). As the daily occultation events are more than one at this hour period, the plot is made separately for every occultation event. Similarly, the Height-Ne figures are the results of the electron density profiles. It can be observed that there is a substantial decrease of the F2 layer peak density on May 9 when compared with other days and that the maximum reduction is approximately 3×10^4 el/cm^3.

Figure 10 shows the variation of geomagnetic index from May 4 to May 12, 2008. As can be observed in the figures, there is a minimum of -24nT Dst index in this period of time (May 5). It means there is only a minor degree of geomagnetic storms in this period. So we can consider the ionosphere changes in this period of time will not be affected by the geomagnetic activity.

As the geomagnetic and solar activity levels were very low from May 4 to May 12, 2008, the decreases in the F2 layer peak density on May 6, 8 and 10 at LT18:00-23:00 can be regarded as the phenomenon of ionospheric disturbances before the earthquake.

A comparison of the results from a single occultation event show that the F2 layer peak density for May 6, 8 and 10 (LT18:00-23:00) and May 9 (LT00:00-05:00) all decrease. As the geomagnetic and solar activity levels were very low from May 4 to May 12, 2008, these decreases can be regarded as the phenomenon of ionospheric disturbances before the earthquake.

From the results above, it can be observed that although ionospheric occultation sounding has advantages such as global coverage, a high vertical resolution and a near real-time signal processing, the number of occultation events is limited and the time resolution of the occultation ionospheric inversion results is still very low. Therefore, we cannot obtain a continuous change of NmF2. For the Wenchuan earthquake, there are several occultation events that occurred at a similar time near the epicenter that can be used for comparisons, and the earthquake-ionosphere anomalies can barely be observed. However, for the Yushu earthquake, which occurred on April 14, 2010, earthquake-ionosphere anomaly detection using the occultation data cannot be performed because of the sparseness of occultation events near the epicenter.

In summary, occultation ionospheric inversion can only currently be employed as a supplement for other ionospheric methods, and its data cannot be used independently in research studies for earthquake-ionosphere anomaly detection applications that have a demand for high time resolution.

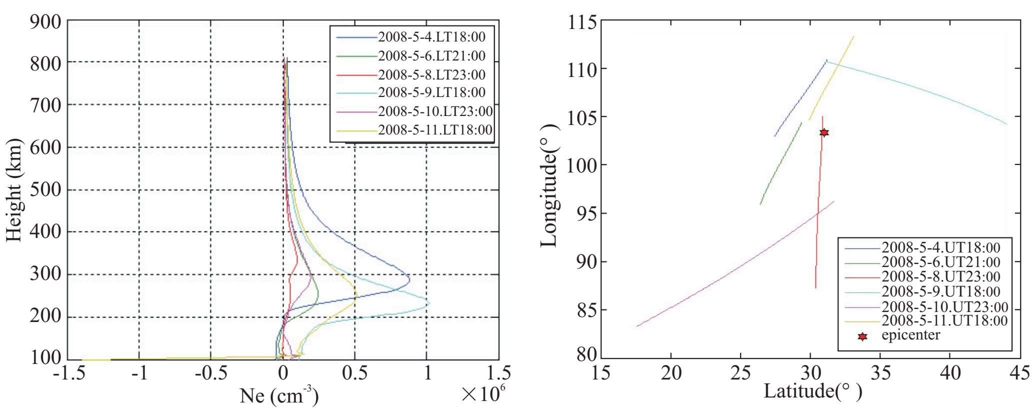

(a) Electron density profiles (b) Occultation tangential point loci

Figure 8 Electron density profiles and occultation tangential point loci (May 4-12, 2008, LT18:00-23:00)

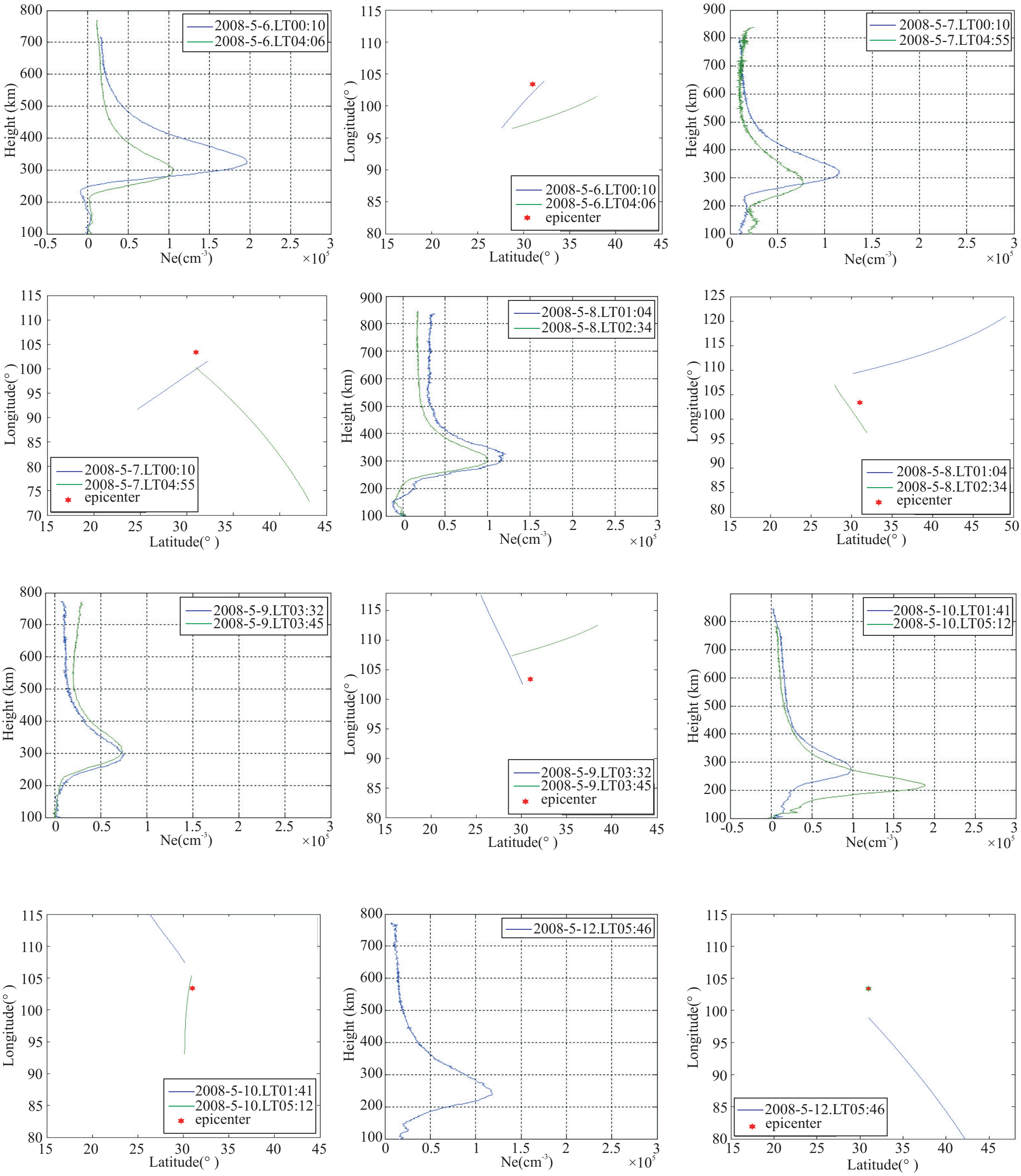

Figure 9 Electron density profiles and occultation tangential point loci (May 4-12, 2008, LT0:00-5:00)

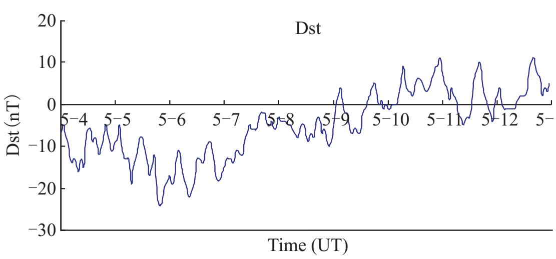

Figure 10 Dst index (May 4-12, 2008)

4 Conclusions

In this study, we analyzed the temporal distribution characteristics of GNSS ionosphere occultation inversion in detail. Earthquake-ionospheric anomalies have also been analyzed by using the example of the Wenchuan earthquake. The results demonstrate the following:

1) The number of occultation events occurring on a specific day is not significant, and there is no rule for the location; the number of matching occultation events occurring on 2 days or on several continuous days at the same time in a similar position is not significant. In addition, the location of the occultation events occurring on 2 different days follows no rules as well. Thus, compared with other traditional means, ionospheric occultation observations have a low temporal resolution.

2) Ionospheric occultation sounding has advantages such as global coverage, which can make up for special areas, such as ocean and polar areas in particular, that lack observational data; however, it can only compare single occultation events to detect abnormal changes in the ionosphere due to its low temporal resolution. Even if making a comparison of single occultation events, adequate occultation events are required near the epicenter a few days before the earthquake for its use. Therefore, ionospheric occultation inversion can only currently be a supplement for other ionospheric means, and its data cannot be used independently in research studies involving earthquake-ionosphere anomaly detection applications, which demand a high temporal resolution.

China is an earthquake-prone country located between two of the world's major earthquake zones: the circus-Pacific seismic belt and the Eurasian seismic zone. Most of the earthquakes that occur in China are shallow-focus earthquakes with focal depths typically 20 km or less. Therefore, China is a country that suffers from some of the most serious earthquake disasters. If short impending predictions of earthquakes are achieved, earthquake damage and loss will be significantly reduced. Ionospheric occultation inversion has its advantages, such as global coverage and a high vertical resolution. Along with the development of GNSS, the global satellite navigation system is no longer a single constellation system; however, a system including GPS, GLONASS, Compass, Galileo constellation, and the number of available satellites will reach more than 100. GNSS ionospheric occultation multi−constellation will increase the number of daily repeated occultation events. Additionally, the establishment of more occultation systems will promote the number of occultation events worldwide. GNSS ionospheric occultation inversion combined with a variety of LEO satellites will significantly improve temporal resolution so that the occultation events may achieve global coverage in one hour or less. It will then be possible to detect earthquake-ionosphere effects though ionospheric occultation inversion, which will be an important contribution to earthquake disaster reduction.

References

[1] Liu J Y, Chuo Y J, Shan S J, Tsai Y B, Chen Y I, Pulinets S A and Yu S B. Pre-earthquake ionospherica nomalies registered by continuous GPSTEC measurements. Annales Geophysicae, 2004, 22: 1585-1593.

[2] Sergey Pulinets. Ionospheric precursors of earthquakes; Recent advances in theory and practical applications. TAO, 2004, 15 (3): 413-435.

[3] Trigunait A, Parrot M, Pulinets S, and Li F., Variations of the ionospheric electron density during the Bhuj seismic event. Annales Geophysicae, 2004, 22: 4123-4131.

[4] Zhao Guoze, Chen Xiaobin and Cai Juntao. Electromagnetic observation by satellite and earthquake prediction. Progress in Geophysics, 2007, 22(3): 667-673. (in Chinese)

[5] Xia Yaqin, Liu Chengyan and Li Junzhi. A study of pre-earthquake ionosphere TEC anomalies upper epicenter. Journal of Beijing University of Technology, 2008, 34(2): 220-224. (in Chinese)

[6] Cai Juntao, Chen Xiaobin, Zhao Guoze, et al. Earthquake precursor: The anomalies in the ionospheric F2 region. Progress in Geophysics, 2007, 22(3): 720-728. (in Chinese)

[7] Li Yong. Possibility to detect Wenchuan *M*8 earthguake by the Earthquake Warning System. Progress in Geophysics, 2008, 23 (3): 969-971. (in Chinese)

[8] Zhang Qiang, Wu Yun, Lin Jian, et al. On Ionospheric TEC Anomaly before earthquake. Journal of Geodesy and Geodynamics, 2007, 27(3): 91-96. (in Chinese)

[9] George A Hajj, Lou C Lee, Xiaoqing Pi, et al. COSMIC GPS ionospheric sensing and space weather. TAO, 2000, 11(1): 235 -272.

[10] Høeg P, Larson GB, Benzon H, et al. GPS atmosphere profiling methods and error assessments, scientific report 98-7, Danish Meteorological Institute, Copenhagen, 1998.